Liquid Crystals

Publication details, including instructions for authors and subscription information:
http://www.informaworld.com/smpp/title~content=t713926090

E.S.R. investigation of helix inversion in induced cholesteric phases

Burkhard Kirste[a]; Günther Scherowsky[b]

[a] Institut für Organische Chemie, Freie Universität Berlin, Berlin, F. R. Germany [b] Institut für Organische Chemie, Technische Universität Berlin, Berlin, F. R. Germany

To cite this Article Kirste, Burkhard and Scherowsky, Günther(1989) 'E.S.R. investigation of helix inversion in induced cholesteric phases', Liquid Crystals, 6: 1, 17 — 29

To link to this Article: DOI: 10.1080/02678298908027319

URL: http://dx.doi.org/10.1080/02678298908027319

LIQUID CRYSTALS, 1989, VOL. 6, NO. 1, 17–29

E.S.R. investigation of helix inversion in induced cholesteric phases

by BURKHARD KIRSTE
Institut für Organische Chemie, Freie Universität Berlin, D-1000 Berlin 33, F.R. Germany

and GÜNTHER SCHEROWSKY
Institut für Organische Chemie, Technische Universität Berlin, D-1000 Berlin 12, F.R. Germany

(*Received 3 January 1989; accepted 24 February 1989*)

The phenomenon of a reversible helix inversion in induced cholesteric mesophases caused by variation of the temperature has been investigated by E.S.R. spectroscopy using the nitroxide radical tempone as spin probe. Chiral esters of optically active (*R*)-(+)-2,2′-dihydroxy-1,1′-binaphthyl were added as dopants to the nematic mixture RO-TN 404. The inversion temperatures and the handedness of the helices were determined. In addition to the distortion parameter which is a measure of the helix pitch, order parameters and rotational correlation times of the spin probe were obtained from line-shape analyses.

1. Introduction

Nematic phases of liquid crystals are converted to cholesteric mesophases by addition of a small amount of a chiral compound. Cholesteric phases exhibit a helical structure which is characterized by the pitch, *P*, and the handedness. The relationship between the properties of the chiral dopant, e.g. the sign and magnitude of the molar rotation, and the molecular twisting power which is responsible for the formation of a cholesteric helix has been investigated in some detail [1]. Measurements of pitch and handedness of the induced cholesteric phase might seem to be an attractive method for chirality investigations. Indeed in the range of limited structural variations in classes of compounds having one asymmetric centre it was found possible to correlate the absolute configuration to the handedness of the induced helix [2–5]. However, a completely general correlation between the chirality of the helix and the absolute configuration of the chiral point does not exist. Thus, the helical screw sense may even be reversed when the same chiral compound is added to different nematic mixtures [6]. A helix inversion caused by increasing the concentration of the chiral dopant has also been observed [7].

The pitch of induced cholesteric phases usually increases with increasing temperature [8], but it may also be temperature independent or even decrease [9]. Recently, chiral dopants were discovered which induce cholesteric phases with an unusual temperature dependence of the helical pitch. Even in systems containing only one chiral dopant, the phenomenon of a reversible *inversion* of the handedness of the helix caused by variation of the temperature was observed [10]. The inversion temperature was found to be almost independent of the concentration of the chiral compound.

One of us found that the helix inversion in an induced cholesteric phase can be caused by a dopant with axial chirality [11]. A diagram illustrating this effect is

0267-8292/89 $3.00

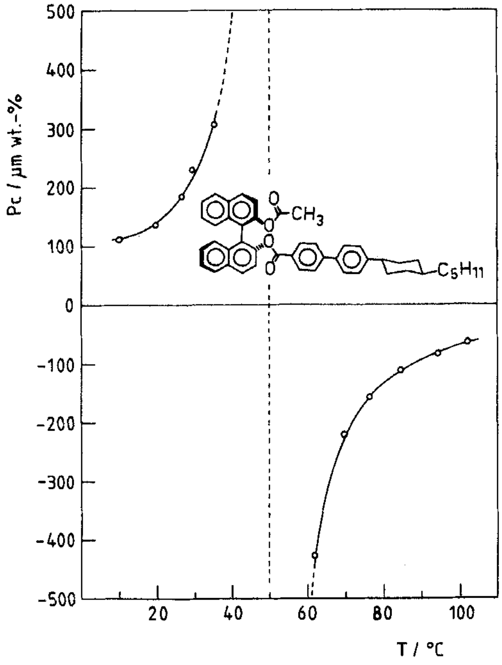

Figure 1. Temperature dependence of the *Pc*-product (pitch · concentration) of compound **2** in RO-TN 404 (c = 1·6 wt %). The helix inversion of the induced cholesteric phase occurs at 50°C.

given in figure 1, which shows the temperature dependence of the pitch. On heating from 10°C the helical pitch increases and becomes infinite above 40°C generating a nematic phase. On further heating, the helical structure reappears but with opposite handedness and decreasing pitch with increasing temperature. In these studies, pitch and handedness of the induced cholesteric phases were determined by the modified Grandjean-Cano method [12, 13], i.e. by optical measurements. As has been demonstrated by Luckhurst and Smith, weakly cholesteric systems can also be studied by E.S.R. spectroscopy provided that a paramagnetic spin probe, e.g. a nitroxide radical is used as a reporter [14, 15]. The E.S.R. technique offers several advantages, because order parameters and dynamic characteristics are accessible from the spectra, in addition to the pitch [16]. Of course, these data refer to the probe molecules and therefore carry only indirect information about the properties of the mesophase [17].

In the present paper we report the investigation of helix inversion in induced cholesteric phases by means of the spin probe technique.

2. Experimental

2.1. *Preparation of samples*

Two optically active diesters (**1** and **2**, see the formulae in figures 2 and 3, respectively) of (*R*)-(+)-2,2′-dihydroxy-1,1′-binaphthyl were used as chiral dopants; their synthesis will be described elsewhere [18]. (**2**: m.p., 121·5–122·5°C, $[\alpha]_{D23}$ = +84·4° [c = 1·5 in $CHCl_3$]; **1** is not crystalline.) Up to 9 wt % of these dopants were dissolved in the nematic mixture RO-TN 404 [T_{NI} = 105°C] from Hoffmann-La Roche to induce the cholesteric phases. The nitroxide radical 4-oxo-2,2,6,6-tetramethylpiperidin-1-oxyl (tempone or tanone) was added as a spin probe in a concentration of c. 5×10^{-4} mol/l. Although this spin probe does not achieve high degrees of ordering in liquid-crystalline solutions, it offers several advantages. Thus, the molecule is not chiral, its E.S.R. spectral lines are fairly narrow, and complications caused by slow tumbling can be neglected even in rather viscous solutions [19]. In some experiments 1 wt % of (−)-cholesteryl chloride was added as an additional dopant. For E.S.R. measurements, the mixtures were transferred to thin-walled cylindrical Pyrex sample tubes (3·3 mm o.d., 2·8 mm i.d.). Samples were deoxygenated by warming them and flushing with purified nitrogen.

2.2. *Instrumentation*

X-band E.S.R. spectra were recorded on a Bruker ER 220D E.S.R. spectrometer which was stabilized by means of a field-frequency lock (Bruker ER 033). The microwave frequency was measured with an HP 5340 A frequency counter and the magnetic field strength ($B_0 \approx 0{\cdot}34$ T) with a Bruker B-NM12 N.M.R. gaussmeter. In g factor measurements, field gradients were corrected for by replacing the sample with a reference compound (phenalenyl in toluene, $g = 2{\cdot}00262$). The temperature of the sample was adjusted by using a temperature control unit (Bruker VT-1000) and checked by means of a thermocouple. E.S.R. spectra were accumulated by using a Nicolet 1170 signal averager employing 1 K data points and afterwards transferred to a minicomputer (HP 1000/A600 or Comtec AT286/10). These computers were used to fit the spectra by means of iterative least-squares procedure [20].

3. Results and discussion

3.1. *E.S.R. measurements*

In the first series of measurements, E.S.R. spectra of a solution of tempone (c. 5×10^{-4} mol/l) in the nematic mixture RO-TN 404 were recorded in the nematic phase as well as in the isotropic phase. The observed three line patterns are typical for nitroxide radicals [21]. Spectra obtained in nematic phases differ from the isotropic spectra because of anisotropic magnetic contributions, i.e. g factor shifts, Δg, and hyperfine shifts, Δa, [22]. These shifts increase with decreasing temperature because of increasing ordering. Nematic phases are uniaxial and there is a unique direction for the alignment of the solvent (the director) and the solutes which coincides with the direction of the external magnetic field (assuming positive diamagnetic anisotropy $\Delta\chi$ as in the present case). In consequence single crystal type spectra are observed.

In the second series of measurements, E.S.R. spectra of a solution of tempone (c. 5×10^{-4} mol/l) and 3·6 wt % of the chiral 2,2′-dihydroxy-1,1′-binaphthyl diester 1 in RO-TN 404 were recorded at a series of temperatures (285–385 K). Three of these spectra are shown in figure 2 (left hand side). At low temperatures (see, e.g., the spectrum recorded at 295 K), an E.S.R. spectrum with a powder-type pattern is observed. The spectral appearance changes drastically with variation in temperature and above 305 K (e.g. at 335 K) a simple single crystal type pattern is obtained. However, at still higher temperatures (above 345 K) a powder pattern reappears. In the isotropic phase (above c. 380 K), the typical three line pattern is again observed. In principle, this behaviour is reversible. However, on cooling the sample below 305 K in the magnetic field (0·34 T) the powder pattern does not form spontaneously but only after the field has been switched off for a short time.

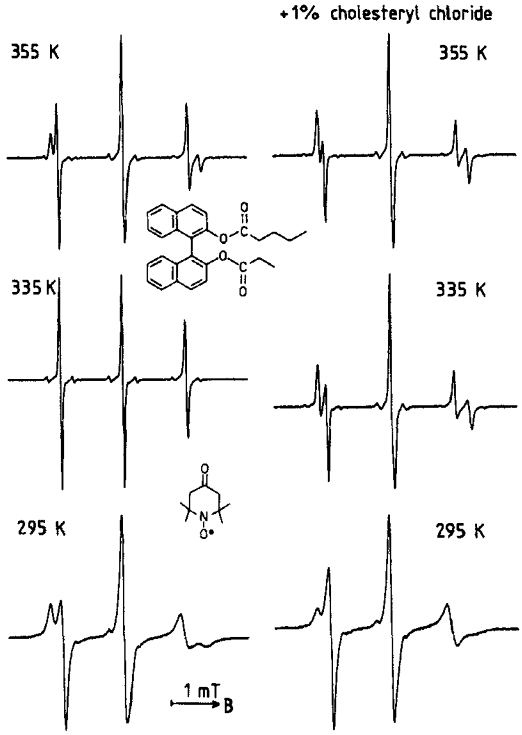

Figure 2. Left hand side: E.S.R. spectra of tempone in RO-TN 404 doped with 3·6 wt % of 1. Right hand side: E.S.R. spectra of the same sample after addition of 1 wt % of (−)-cholesteryl chloride.

The particular powder patterns observed at low (e.g. at 295 K) and at high temperatures (e.g. at 355 K) are characteristic of weakly cholesteric systems [14]. The helix axis of cholesteric phases (with $\Delta\chi > 0$) is aligned perpendicular to the magnetic field direction. The local director is always perpendicular to the helix axis but it circulates periodically around this axis. Consequently there is a spatial variation of the angle γ between the local director and the field axis. In an unperturbed cholesteric helix, all angles between 0° and 360° are equally likely giving rise to a two dimensional distribution of the director. In the usual first derivative display, the E.S.R. spectrum is dominated by the two spectra associated with the director parallel ($\gamma = 0°$) and perpendicular ($\gamma = 90°$) to the magnetic field [15]. In weakly cholesteric systems, the magnetic field causes a partial unwinding of the helix, and the relative contribution of non-parallel orientations decreases [14]. In the limiting case, the helix is completely unwound and a nematic phase is formed.

In the present case (see figure 2, left hand side), the spectra observed at 295 K and at 355 K correspond to distorted cholesteric phases. Since $\tilde{a}_N$ (90°) > $\tilde{a}_N$ (0°) for tempone, the outer wings of the two hyperfine shifted E.S.R. components belong to perpendicular orientations, whereas the inner peaks belong to the parallel orientation. In the two spectra under consideration, the perpendicular features are clearly less intense than the parallel features. In the intermediate temperature range (e.g. at 335 K), only parallel features are observed, i.e. the phase is nematic. Since the relative intensity of the perpendicular features increases with decreasing pitch of the unperturbed cholesteric helix [16], the interpretation of the temperature dependence of the spectra is as follows. Starting at low temperatures (285 K), the pitch of the cholesteric phase increases with increasing temperature. Then there is a gap between about 305 K and 345 K where the sample exhibits a nematic phase when in the magnetic field (0·34 T). Above 345 K, a cholesteric phase forms again, but now the pitch decreases with increasing temperature. This is just the behaviour which is illustrated in figure 1.

The E.S.R. spectra convey no direct evidence of the handedness of the helix. However, the helical screw sense can be determined by adding a dopant known to induce a certain handedness. For instance, (−)-cholesteryl chloride usually induces right handed (*P*) helices, e.g. in MBBA [1]. However, optical measurements performed at room temperature and above have established that an *M* helix is induced in the nematic mixture RO-TN 404. Thus, in a third series of measurements 1 wt % of (−)-cholesteryl chloride was added. Three spectra recorded at corresponding temperatures are shown in figure 2 (right hand side). Obviously the cholesteric character of the mixture is enhanced at high temperatures but reduced at low temperatures by adding (−)-cholesteryl chloride. Therefore we conclude that **1** induces an *M* helix in RO-TN 404 at high temperatures but a *P* helix at low temperatures. Thus, the E.S.R. measurements prove the phenomenon of a temperature dependent helix inversion, confirming previous investigations using optical techniques [11].

In the proximity of the inversion temperature, the helical twisting power exhibited by **1** is rather small. Hence the cholesteric induction cannot compete with the perturbing effect of the magnetic field (0·34 T) for the mixture studied (3·6 wt % of **1** in RO-TN 404) over a fairly wide temperature range (305–345 K). In order to reduce this gap, we have studied a second chiral dopant (**2**) which allows us to employ higher concentrations. Thus, in a fourth series of measurements a mixture of tempone and 8·6 wt % of **2** in RO-TN 404 was investigated. Three E.S.R. spectra are reproduced in figure 3 (left hand side). The behaviour is analogous to that of **1**, but now the intermediate nematic phase extends only from about 310 K to 320 K. Subsequently this mixture was diluted by adding RO-TN 404, yielding a concentration of 4·1 wt % of **2**. As expected, the strength of the cholesteric induction is reduced correspondingly and the intermediate nematic range now extends between about 310 K and 330 K (fifth series). Thus, by diluting the sample by a factor of two the inversion temperature is increased by approximately 5 K. The handedness of the helices was established again by adding 1 wt % of (−)-cholesteryl chloride to this mixture (sixth series). In analogy to **1**, the phase exhibits an *M* helix at high temperature and a *P* helix at low temperature.

3.2. *Computer simulations*

The E.S.R. spectra of tempone in weakly cholesteric systems carry information about g factors and g factor shifts, Δg, the nitrogen hyperfine coupling constant a_{N} and its anisotropic shift, Δa_{N}, the distortion parameter K describing the partial unwinding of the cholesteric helix by the field, and the linewidths and their angular dependences. The prominent features of the hyperfine shifted peaks can be associated with parallel ($\gamma = 0°$) and perpendicular ($\gamma = 90°$) director orientations. Therefore approximate g factor and hyperfine data can be extracted directly from the spectra [22],

$$\tilde{A}_{\parallel} = \tilde{a}(0°) = a + \Delta a, \tag{1}$$

$$\tilde{A}_{\perp} = \tilde{a}(90°) = a - \Delta a/2, \tag{2}$$

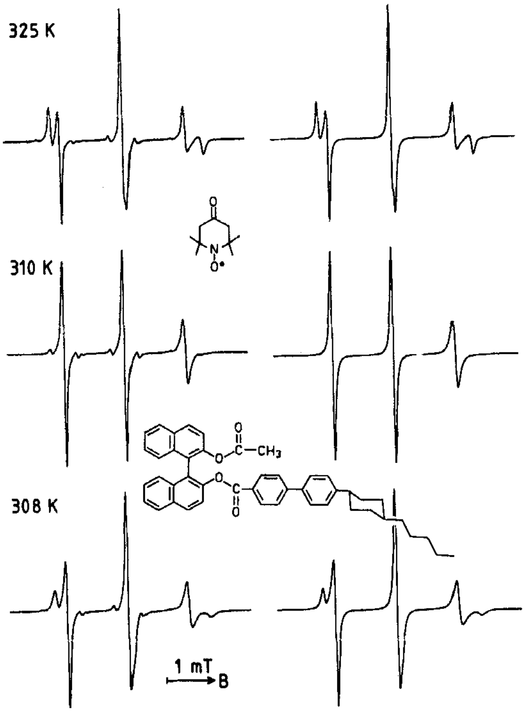

Figure 3. Left hand side: E.S.R. spectra of tempone in RO-TN 404 doped with 8·6 wt % of 2. Right hand side: Computer simulated E.S.R. spectra calculated with distortion parameters K of 0·91 (308 K), 1 (310 K), and 0·73 (325 K). (Further parameters at 325 K: $\tilde{g}_{\parallel} = 2{\cdot}00634$, $\tilde{g}_{\perp} = 2{\cdot}00587$, $\tilde{A}_{\parallel} = 35{\cdot}81$ MHz, $\tilde{A}_{\perp} = 44{\cdot}05$ MHz, linewidth parameters [mT] $A^*_{0°} = 0{\cdot}039$, $A^*_{90°} = 0{\cdot}050$, $B^*_{0°} = -0{\cdot}010$, $B^*_{90°} = -0{\cdot}009$, $C^*_{0°} = 0{\cdot}010$, and $C^*_{90°} = 0{\cdot}008$.)

where $\tilde{A}_{\parallel}$ and $\tilde{A}_{\perp}$ are the principal values of the partially averaged (nitrogen) hyperfine tensor; analogous equations apply to the g factor. To obtain reliable values for the distortion parameter K and the angle-dependent linewidths it is necessary to compare the experimental E.S.R. spectra with computer simulated spectra. The theory required for performing simulations of polyliquid crystalline E.S.R. spectra has been described by Gottarelli *et al.* [16], and their procedure was followed in the present study. E.S.R. spectra were calculated for a series of orientations, i.e., the angle γ was varied from 0° to 90° in steps of about 5°, taking the M_I and angular dependence of the linewidths into account. These spectra were summed up by using a weighting factor $P(\gamma)$ [14]

$$P(\gamma) = (1 - K^2 \cos^2 \gamma)^{-1/2} \left[\int_0^{\pi/2} (1 - K^2 \cos^2 \gamma)^{-1/2} \, d\gamma \right]^{-1}. \tag{3}$$

The approximations made in [16] were also adopted in the present investigation. In particular, satellite peaks from isotopomers with ^{13}C and ^{15}N in natural abundance were not taken into account, the validity of the Redfield limit was assumed (fast tumbling regime), and the lineshape was taken to be purely lorentzian. Since unresolved proton hyperfine interactions give rise to inhomogeneous line broadening with gaussian line shapes, the latter approximation prevents perfect agreement between simulated and experimental spectra.

Because several parameters required to perform the simulations are not known *a priori* and have to be guessed, automatic curve fitting was used to refine the parameters. Specifically, the Monte Carlo method described in a previous paper was employed [20]. Thus, the parameters were varied by small but random amounts, and the new set was retained if a better fit in terms of the least-squares criterion was obtained. The fitting procedure turned out to be rather tedious, mainly because of counteracting effects of variations of the distortion parameter, K, and the linewidth parameters. Moreover, all of the parameters are strongly temperature dependent. Altogether, about 90 experimental spectra were processed. The quality of the fit is illustrated by the three computer simulated spectra shown in figure 3 (right hand side). As stated previously [16], the shape of the E.S.R. spectrum is sensitive to the distortion parameter, K, in the range $0{\cdot}7 \leqslant |K| < 1$. Note that $K = 0$ corresponds to an undistorted cholesteric helix, whereas $K = 1$ is for a nematic phase (i.e. $\gamma = 0°$ throughout the sample). Although, in principle, E.S.R. spectra from cholesteric phases contain information about the complete angular dependence, reliable values for the linewidth parameters can only be obtained for $\gamma = 0°$ and $\gamma = 90°$ (or only for 0° when K approaches one). This is a consequence of the powder line-shape. For detailed studies of angle dependent properties, cholesteric phases are therefore less suited than smectic A phases [23].

3.3. *Distortion parameter*

The most interesting parameter in the present investigation is certainly the distortion parameter, K, because it is related to the pitch of the cholesteric helix by the following expression (SI system) [16]

$$K = (P_0 B/\pi^2)\,(\Delta\chi/\mu_0 K_2)^{1/2}\,E(K), \tag{4}$$

where P_0 is the pitch of the undistorted helix, B is the magnetic flux density, $\Delta\chi$ is the anisotropy of the diamagnetic susceptibility, K_2 is the scalar twist elastic constant of the mixture and $E(K)$ is an elliptic integral of the second kind

$$E(K) = \int_0^{\pi/2} (1 - K^2 \sin^2\gamma)^{1/2}\,d\gamma. \tag{5}$$

Thus, although the pitch P_0 is proportional to the quantity $K/E(K)$, knowledge of the material constants $\Delta\chi$ and K_2 and their temperature dependences is required for the determination of absolute values. However, plots of $E(K)/K$ versus temperature are well suited for comparing the properties of different cholesteric mixtures. Note that this quantity is proportional to the product of the molecular twisting power, β, and the molar concentration, c,

$$E(K)/K \sim P_0^{-1} = \beta c. \tag{6}$$

The results are given in figure 4. Because of the condition $0{\cdot}7 \leqslant |K| < 1$, reliable values of $E(K)/K$ can only be obtained for $1 < |E(K)/K| < 2$. The E.S.R. lineshape is a function of K^2 and hence independent of the sign of K, but the method employed for the determination of the sign, i.e. the handedness of the helix, has been described earlier. The useful range of data points extends from $E(K)/(K) \approx -2$ to 2 with a gap between -1 and 1. This gap corresponds to the region of complete unwinding of the cholesteric helix by the magnetic field, i.e. a nematic range. It is noteworthy that the data show an essentially linear dependence on temperature within the accessible

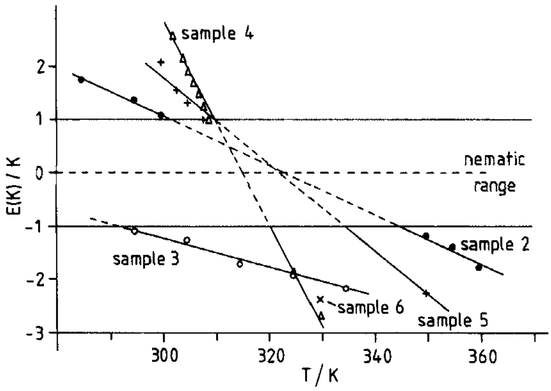

Figure 4. Temperature dependences of the function $E(K)/K$ of the distortion parameter, K, for different samples, see text and equations (3)–(5). Note that this function is not defined for values between -1 and 1 corresponding to complete unwinding of the cholesteric helix by the magnetic field.

range. The inversion temperatures can be determined by interpolation, yielding 324 K for sample 2 (3·6 wt % of **1** in RO-TN 404), 315 K for sample 4 (8·6 wt % of **2**), and 322 K for sample 5 (4·1 wt % of **2**). In accord with equation (6), the slope is proportional to the concentration ($m_5/m_4 = 0{\cdot}45$).

With the material constants of RO-TN 404 which have been measured at 22°C, $K_1 = 16{\cdot}5 \times 10^{-12}$ N, $K_2 = 7{\cdot}5 \times 10^{-12}$ N, $K_3 = 23{\cdot}4 \times 10^{-12}$ N, $\Delta n = 0{\cdot}260$, and $\Delta\chi = 1{\cdot}86 \times 10^{-6}$ (SI units) [24], the pitch of the cholesteric samples can be calculated from equation (4) ($B = 0{\cdot}34$ T). Thus, the following values for the unperturbed pitch P_0 at 295 K are obtained: 47·6 μm (P, sample 2), 58·6 μm (M, sample 3), and 23·3 μm (P, sample 5). Consequently, the molecular twisting power β (see equation (6)) is 250 m^2/mol for compound **1** and 690 m^2/mol for compound **2** in RO-TN 404 at 295 K.

3.4. *Order parameters and dynamic behaviour*

The anisotropic g factor shifts, Δg, and nitrogen hyperfine shifts, Δa_N, are given by the inner products of the ordering matrix $\mathcal{O}$ of the spin probe and the **g** tensor or the hyperfine tensor $\mathbf{A}_N$, respectively. In a principal axis system we obtain in cartesian notation [22]:

$$\Delta a_N = \mathcal{O}_{zz}(A_{zz}^N - a_{iso}^N) + (1/3)(\mathcal{O}_{xx} - \mathcal{O}_{yy})(A_{xx}^N - A_{yy}^N), \qquad (7)$$

$$\Delta g = \mathcal{O}_{zz}(g_{zz} - g_{iso}) + (1/3)(\mathcal{O}_{xx} - \mathcal{O}_{yy})(g_{xx} - g_{yy}). \qquad (8)$$

Using the axis system defined by Gottarelli *et al.* [16] (y axis along the N–O bond direction, x axis perpendicular to the molecular plane) and tensor data from [25] ($A_{xx} = 3{\cdot}345$ mT, $A_{yy} = 0{\cdot}41$ mT, $A_{zz} = 0{\cdot}61$ mT, $g_{xx} = 2{\cdot}0022$, $g_{yy} = 2{\cdot}0096$, and $g_{zz} = 2{\cdot}0063$), the order parameters $\bar{P}_2$ and $\bar{P}_{2,2}$,

$$\bar{P}_2 = \mathcal{O}_{zz}, \qquad (9)$$

$$\bar{P}_{2,2} = (1/6)^{1/2}(\mathcal{O}_{xx} - \mathcal{O}_{yy}), \qquad (10)$$

can be calculated from the measured Δg and Δa_N values. For the systems studied, Δg was found to be proportional to Δa_N within experimental accuracy, therefore $\bar{P}_{2,2} \sim \bar{P}_2$ (this need not be true in general [26]). The main order parameter $\bar{P}_2$ refers

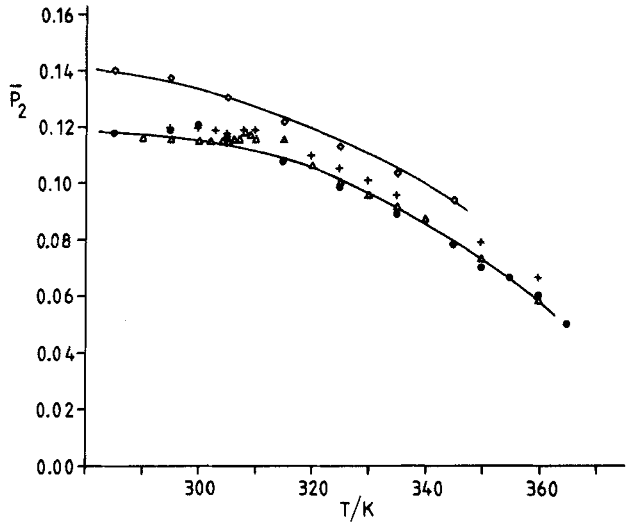

Figure 5. Temperature dependence of the order parameter, $\bar{P}_2$, for different samples, see text. $\bar{P}_2$ was calculated from $-\Delta a_N/55{\cdot}0$ MHz ($\bar{P}_{2,2} = -0{\cdot}46\bar{P}_2$) and refers to the probe molecules, tempone. ◇ = sample 1; ● = sample 2; △ = sample 4; + = sample 5.

to the degree of ordering of the solute and is certainly much smaller than the order parameter of the phase, but it can reasonably be assumed that it is proportional to the latter. A plot of the order parameters $\bar{P}_2$, calculated from $-\Delta a_N/55{\cdot}0$ MHz, is given in figure 5 ($\bar{P}_{2,2} = -0{\cdot}46\bar{P}_2$). All curves exhibit the typical temperature variation of order parameters of nematic phases. The substantial amount of 4–9 wt % of added dopant markedly decreases the order parameter by up to 20 per cent.

The E.S.R. linewidths (T_2^{-1}) depend on the magnetic spin quantum number of the ^{14}N nucleus, M_I,

$$T_2^{-1} = A + BM_I + CM_I^2, \qquad (11)$$

with angle dependent linewidth parameters A, B, and C. The fitting procedure described here does not yield the true parameters but values which include the broadening due to unresolved methyl proton hyperfine splittings and field inhomogeneities. The inhomogeneous line broadening affects mainly the parameter A but causes only minor errors in the evaluation of the parameters B and C. The apparent linewidth parameters A^*, B^*, and C^* determined for sample 1 (tempone in pure RO-TN 404, $\gamma = 0°$) and sample 4 (containing 8·6 per cent of **2**, $\gamma = 0°$ and 90°) are depicted in figure 6. The temperature dependence of these parameters is not very pronounced between 320 K and 360 K, but their magnitudes increase strongly below 315 K.

In isotropic solutions, the linewidth parameters depend on the dipolar hyperfine tensor and/or the g tensor and on the rotational correlation times [27, 28]. Hence increasing linewidths with decreasing temperature are due to increasing viscosity η, which is related to the rotational correlation time τ_R by the Stokes–Einstein equation

$$\tau_R = V_{\text{eff}}\eta/(kT), \qquad (12)$$

where V_{eff} is the effective volume of the tumbling molecule. In liquid-crystalline solutions, the angle dependence of the linewidth parameters has to be taken into

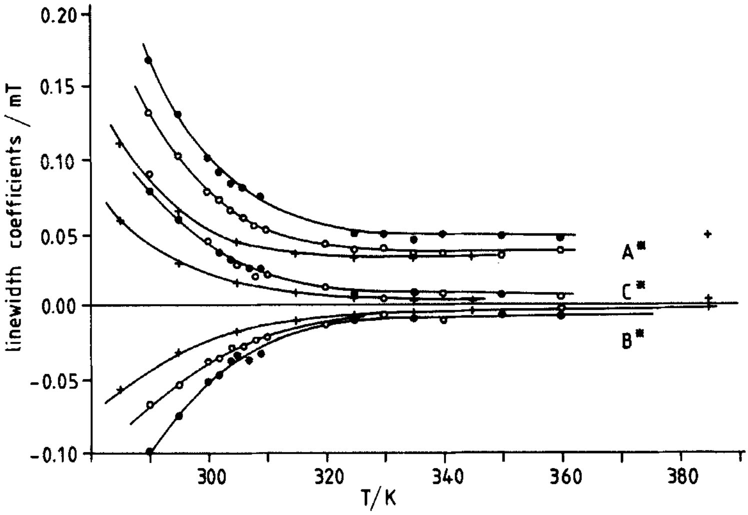

Figure 6. Temperature dependences of the apparent E.S.R. linewidth parameters A^*, B^*, and C^* for samples 1 ($\gamma = 0°$) indicated by + and 4 ($\gamma = 0°$ represented by ○ and 90° shown by ●).

account via

$$B(\gamma) = B_0 + B_2 P_2(\cos\gamma) + B_4 P_4(\cos\gamma), \tag{13}$$

where $P_2(\cos\gamma)$ and $P_4(\cos\gamma)$ are Legendre polynomials; analogous equations apply to the parameters A and C [29, 30]. The parameters B_0, B_2, and B_4 in equation (13) depend on the dipolar hyperfine and g tensors, the orientational order parameter $\bar{P}_2$, the higher order parameter $\bar{P}_4$ and the rotational correlation times τ_0 and τ_2, where τ_0 describes the reorientation of the long molecular axis (the z axis) and τ_2 rotation about this axis.

Apparently, the effects of increasing order and increasing viscosity roughly compensate each other in the temperature range between 320 K and 360 K. On the other hand, the variation of the order parameters is quite small below 310 K (see figure 5). Therefore the strong increase of the linewidths below 310 K (see figure 6) reflects a corresponding increase in viscosity. It is noteworthy that the addition of dopant (8·6 per cent of **2** in sample 4) markedly increases the viscosity of the mixture.

For the extraction of the true linewidth parameters A from the measured A^* values (*vide supra*), knowledge of the methyl proton hyperfine splittings is required. Although, in principle, the components of the partially averaged $\tilde{A}_{\mathrm{Me}}$ tensor can be determined by ENDOR spectroscopy, attempted ENDOR measurements on tempone in the cholesteric phases under investigation were not successful. Alternatively, the line broadening due to unresolved hyperfine splittings can be estimated from the order parameters and published molecular tensor data [16, 31]. This procedure yields inhomogeneous linewidth contributions of $X(0°) = 0{\cdot}030$ mT and $X(90°) = 0{\cdot}050$ mT at 360 K and of $X(0°) = 0{\cdot}018$ mT and $X(90°) = 0{\cdot}057$ mT at 310 K and below.

The rotational correlation times τ_0 and τ_2 can be evaluated from the equations given in [29], the molecular tensor data [16], the linewidth parameters, and the order

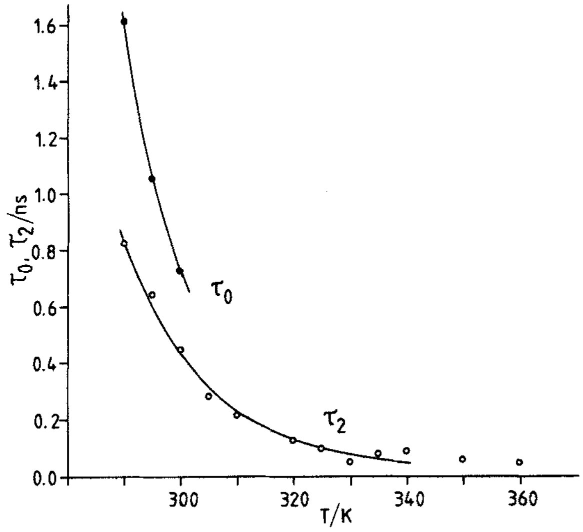

Figure 7. Temperature dependences of the rotational correlation times τ_0 and τ_2 of tempone in sample 4. The lower curve represents a least-squares fit to the experimental τ_2 data.

parameters $\bar{P}_2$ and $\bar{P}_4$. Since the order parameter $\bar{P}_2$ of the tempone spin probe is relatively small (see figure 5), the fourth rank order parameter $\bar{P}_4$ is almost negligibly small and has been estimated from its theoretical relation to $\bar{P}_2$ [32]. In principle, τ_0 and τ_2 can be extracted by means of a multilinear regression. The linewidth parameters A were not used in this procedure because of the problems mentioned previously. Actually reasonable values for both τ_0 and τ_2 (with $\tau_0 \approx 2\tau_2$) were obtained in the temperature range between 290 and 300 K (sample 4). The values of A calculated with these data are in accord with the experimental data when the line broadening due to unresolved proton hyperfine splittings is taken into account. Since above 300 K the regression yielded a wide variation in values for τ_0 when both parameters were allowed to vary, a constant ratio of $\tau_0 = 2\tau_2$ was assumed and only τ_2 treated as an independent variable. This ratio is also in agreement with previous findings [16]. The temperature dependence of the rotational correlation times of tempone in sample 4 (RO-TN 404 with 8·6 wt.-per cent of **2**) is shown in figure 7. The lower curve represents the best fit to the experimental τ_2 data, assuming that $\ln \tau_2$ is a linear function of $1/T$. The apparent activation energy is $48 \pm 3\,\mathrm{kJ\,mol^{-1}}$.

4. Conclusion

We have demonstrated that the phenomenon of helix inversion in induced cholesteric mesophases with temperature variation, previously detected by optical measurements, can also be studied by E.S.R. techniques. A qualitative application of the method is quick and simple, since the powder E.S.R. lineshape obtained from a cholesteric phase is quite different from the single crystal type line shape characteristic of nematic phases. The inversion temperature and crude estimates of the helix pitch can be obtained easily, and the handedness can be determined by adding a reference compound.

Moreover, the E.S.R. method allows the determination of order parameters and of rotational correlation times and hence the microviscosity of the phase. For an accurate evaluation of the rotational correlation times and the distortion factor which characterizes the pitch, detailed lineshape analyses must be performed, however. Since substantial amounts of chiral dopant (up to 9 wt %) were added in the present study, a substantial decrease of the order parameters and an even more pronounced increase of the viscosity of the mixture was found.

An explanation for the observed helix inversion is not easily given. It may be speculated that temperature-dependent conformational changes of the chiral dopant are responsible for this behaviour. An equilibrium between cisoid and transoid conformations of 1,1′-binaphthyl derivatives has in fact been postulated in a previous study by Naciri *et al.* [33].

We would like to thank Hoffmann-La Roche for supplying us with nematic liquid crystals and Dr. M. Schadt for the measurement of the material constants of RO-TN 404. Financial support by the Deutsche Forschungsgemeinschaft (Schwerpunktprogramm 'Thermotrope Flüssigkristalle') and the Fonds der Chemischen Industrie is gratefully acknowledged.

References

[1] SOLLADIÉ, G., and ZIMMERMANN, R. G., 1984, *Angew. Chem.*, **96**, 335; 1984, *Angew. Chem., Int. Ed. Engl.*, **23**, 348.

[2] GOTTARELLI, G., SAMORI, B., MARZOCCHI, S., and STREMMENOS, C., 1975, *Tetrahedron Lett.*, **24**, 1981.

[3] KRABBE, H.-J., HEGGEMEIER, H., SCHRADER, B., and KORTE, E. H., 1978, *J. chem. Res.* (S), p. 238; 1978, *J. chem. Res.* (M), p. 3023.

[4] RINALDI, P. L., and WILK, M., 1983, *J. org. Chem.*, **48**, 2141.

[5] DRAKE, A. F., GOTTARELLI, G., and SPADA, G. P., 1984, *Chem. Phys. Lett.*, **110**, 630.

[6] SIEMENSMEYER, K., and STEGEMEYER, H., 1986, *XI Int. Liquid Crystal Conf.*, Berkeley.

[7] STEGEMEYER, H., and FINKELMANN, H., 1973, *Chem. Phys. Lett.*, **23**, 227.

[8] STEGEMEYER, H., and FINKELMANN, H., 1975, *Naturwissenschaften*, **62**, 436.

[9] HEPPKE, G., LÖTZSCH, D., and OESTREICHER, F., 1986, *Z. Naturf.* (*a*), **41**, 1214.

[10] HEPPKE, G., LÖTZSCH, D., and OESTREICHER, F., 1987, *Z. Naturf.* (*a*), **42**, 279.

[11] SCHEROWSKY, G., 1986, presented in part at the XI Int. Liquid Crystal Conf., Berkeley.

[12] HEPPKE, G., and OESTREICHER, F., 1977, *Z. Naturf.* (*a*), **32**, 899.

[13] HEPPKE, G., and OESTREICHER, F., 1978, *Molec. Crystals liq. Crystals Lett.*, **41**, 245.

[14] LUCKHURST, G. R., and SMITH, H. J., 1973, *Molec. Crystals liq. Crystals*, **20**, 319.

[15] LUCKHURST, G. R., and SMITH, H. J., 1975, *Molec. Phys.*, **29**, 317.

[16] GOTTARELLI, G., PEDULLI, G. F., and ZANNONI, C., 1982, *Chem. Phys.*, **64**, 143.

[17] DALMOLEN, L. G. P., EGBERTS, E., and DE JEU, W. H., 1984, *J. Phys., Paris*, **45**, 129.

[18] SCHEROWSKY, G., and KUTZBORSKI, A. (to be published).

[19] FREED, J. H., and POLNASZEK, C. F., 1975, *J. phys. Chem.*, **79**, 2283. LIN, W. J., and FREED, J. H., 1979, *J. phys. Chem.*, **83**, 379.

[20] KIRSTE, B., 1987, *J. magn. Reson.*, **73**, 213.

[21] BERLINER, L. J. (editor), 1976, *Spin Labeling. Theory and Applications*, Vol. 1 (Academic Press).

[22] FALLE, H. R., and LUCKHURST, G. R., 1970, *J. magn. Reson.*, **3**, 161.

[23] KIRSTE, B., 1987, *Z. Naturf.* (*a*), **42**, 1296.

[24] SCHADT, M. (Hoffmann-La Roche) (personal communication).

[25] HWANG, J. S., MASON, R. P., HWANG, L. P., and FREED, J. H., 1975, *J. phys. Chem.*, **79**, 489.

[26] GHOSH, S. K., RICCHIUTO, A., PANATTA, A., and INDOVINA, P. L., 1986, *Nuovo Cim. Soc. Ital. Fis.* D, **D7**, 825.

[27] FREED, J. H., and FRAENKEL, G. K., 1963, *J. chem. Phys.*, **39**, 326.

[28] Hudson, A., and Luckhurst, G. R., 1969, *Chem. Rev.*, **69**, 191.
[29] Luckhurst, G. R., Setaka, M., and Zannoni, C., 1974, *Molec. Phys.*, **28**, 49.
[30] Luckhurst, G. R., Setaka, M., and Yeates, R. N., 1981, *J. magn. Reson.*, **42**, 351.
[31] Polnaszek, C. F., 1975, Ph.D. Thesis, Cornell University, U.S.A.
[32] Luckhurst, G. R., and Yeates, R. N., 1976, *J. chem. Soc., Faraday Trans. II*, **72**, 996.
[33] Naciri, J., Spada, G. P., Gottarelli, G., and Weiss, R. G., 1987, *J. Am. chem. Soc.*, **109**, 4352.